Available online at www.sciencedirect.com
ScienceDirect
Catalysis Today 124 (2007) 133–148
CATALYSIS TODAY
www.elsevier.com/locate/cattod

Titanium dioxide-mediated photocatalysed degradation of few selected organic pollutants in aqueous suspensions

W. Bahnemann [a,1], M. Muneer [b,2,*], M.M. Haque [c]

[a] *Institut fuer Technische Chemie, Universitaet Hannover, Callinstrasse-3, D-30167 Hannover, Germany*
[b] *Centre for Material Science, University of Central Lancashire, Preston PR1 2HE, UK*
[c] *Department of Chemistry, Aligarh Muslim University, Aligarh 202002, India*

Available online 25 April 2007

Abstract

The photocatalytic degradation of maleic hydrazide (**1**), propham (**2**), tebuthiuron (**3**), propachlor (**4**), chlortoluron (**5**), thiram (**6**), phenoxyacetic acid (**7**), 2,4,5-trichlorophenoxy acetic acid (**8**), 4-chlorophenoxy acetic acid (**9**), uracil (**10**), 5-bromouracil (**11**) and bromothymol blue (**12**) have been investigated in aqueous suspensions of titanium dioxide (TiO_2) under a variety of conditions. The degradation was studied by monitoring the change in substrate concentration employing UV spectroscopic analysis technique and depletion in total organic carbon (TOC) content as a function of irradiation time. The degradation kinetics of the compounds were investigated under different conditions, such as types of TiO_2, pH, catalyst concentration, substrate concentration, temperature and in the presence of different electron acceptors, such as hydrogen peroxide (H_2O_2), potassium persulphate ($K_2S_2O_8$), ammonium persulphate $(NH_4)_2S_2O_8$ and potassium bromate ($KBrO_3$) besides molecular oxygen. TiO_2 Degussa P25 was found to be more efficient photocatalyst for the degradation of the model compounds as compared with other photocatalysts. The degradation products were analysed using GC/MS analysis technique and probable pathways for the formation of different products have been proposed.

Keywords: Photocatalytic degradation; Semiconductor; Titanium dioxide; Pesticides

1. Introduction

The control of organic pollutants in water is an important measure in environmental protection. A large amount of chemicals are used in agricultural field for better quality and quantity of the crop. Hence, a wide variety of pesticides are applied on agricultural sites, which due to their chemical stability, resistance to biodegradation and sufficient water solubility penetrate deep into the ground water [1,2]. Their toxicity, stability to natural decomposition and persistence in the environment has been the cause of much concern to the societies and regulation authorities around the world [3]. Wastewater from the textile industry is highly colored and of a complex and variable nature. The large amount of dyestuffs used in dyeing stage of textile manufacturing processes represent an increasing environmental danger due to their refractory nature. The textile dyes and other commercial colorants have emerged as a focus of environmental remediation efforts. These efforts have largely been targeted at removing colorants from wastewater effluents of textile mills and other colorant manufacturers [4–6]. A substantial amount of dyestuff is lost during the dyeing process in the textile industry [7]. The release of those colored wastewaters in the environment is a considerable source of non aesthetic pollution and eutrophication and can originate dangerous byproducts through oxidation, hydrolysis, or other chemical reactions taking place in the wastewater phase [8,9]. Decolorization of dye effluents has therefore acquired increasing attention.

Development of appropriate methods for the degradation of contaminated drinking, ground, surface waters, wastewaters containing toxic or nonbiodegradable compounds is necessary. Among many processes proposed and/or being developed for the destruction of the organic contaminants, biodegradation has

* Corresponding author. Tel.: +44 1772 893578; fax: +44 1772 892996.
E-mail addresses: bahnemann@iftc.uni-hannover.de (W. Bahnemann), MMuneer@uclan.ac.in (M. Muneer), drmmhaque@gmail.com (M.M. Haque).
[1] Tel.: +49 511 7625560; fax: +49 511 7623004.
[2] On leave from the Department of Chemistry, Aligarh Muslim University, Aligarh, India.

0920-5861/$ – see front matter © 2007 Elsevier B.V. All rights reserved.
doi:10.1016/j.cattod.2007.03.031

received the greatest attention. However, many organic chemicals, especially those that are toxic or refractory, are not amendable to microbial degradation. Recently, considerable attention has been focussed on the use of semiconductor as a means to oxidize toxic organic chemicals [10–17]. The photocatalysed degradation of various organic systems employing irradiated TiO_2 is well documented in literature [10]. The initial step in the TiO_2 mediated photocatalysed degradation is proposed to involve the generation of (e^-/h^+) pair leading to the formation of hydroxyl radical and superoxide radical anion (Eqs. (1)–(8)):

$$TiO_2 + h^*\nu \rightarrow TiO_2 + h^+ + e^- \quad (1)$$

$$TiO_2(h^+) + {}^-OH_{(ad)} \rightarrow TiO_2 + {}^\bullet OH_{(ad)} \quad (2)$$

$$TiO_2(h^+) + {}^-OH_{(ad)} \rightarrow TiO_2 + OH_{(ad)} \quad (3)$$

$$TiO_2(e^-) + O_2 \rightarrow TiO_2 + O_2{}^{\bullet -} \quad (4)$$

$$O_2{}^{\bullet -} + H^\oplus \rightarrow HO_2{}^\bullet \quad (5)$$

$$O_2{}^{\bullet -} + HO_2{}^\bullet \rightarrow {}^\bullet OH + O_2 + H_2O_2 \quad (6)$$

$$2HO_2{}^\bullet \rightarrow O_2 + H_2O_2 \quad (7)$$

$$TiO_2(e^-) + H_2O_2 \rightarrow TiO_2 + {}^-OH + {}^\bullet OH \quad (8)$$

It has been suggested that the hydroxyl radicals and superoxide radical anions are the primary oxidizing species in the photocatalytic oxidation processes. These oxidative reactions would result in the degradation of the pollutant and the efficiency of the degradation will depend upon the oxygen concentration, which determines the efficiency with which the conduction band electrons are scavenged and the (e^-/h^+) recombination is prevented. Alternatively, direct absorption of light by the dye, can lead to charge injection from the excited state of the dye to the conduction band of the semiconductor as summarized in the following Eqs. (9)–(10);

$$Dye_{ads} + h\nu \rightarrow Dye^*_{ads}$$

$$Dye^*_{ads} + TiO_2 \rightarrow Dye^+_{ads}{}^\bullet + TiO_2(e^-) \quad (10)$$

The consumption of water for processing 1 kg of textile goods varies from 10 to 300 L, depending on the nature of the fiber, form of textile goods and processing. Taking a conservative figure of 100 L of water per kilogram the amount of wastewater generated by the textile industry works out to a gigantic 4500 million kiloliters. Handling of such a huge quantity of wastewater is not only a difficult task but also a highly significant risk in maintaining the supply of safe drinking water. About 10,000 different dyes and pigments exist and over 7×10^5 tonnes of these are produced annually worldwide. Besides this the water also contaminated through various other sources like chemical spills, industrial effluents, agricultural runoff, etc. The organic compounds due to chemical resistivity, resistance to biodegradation and with sufficient water solubility penetrate deep into the ground water leading to surface and underground water contamination. This contaminated water should be purified before it is used for any other purpose. Hence, an attempt is made to study the degradation kinetics of various priority organic pollutants under different reaction parameters in order to get the optimized degradation condition, which is very essential for any practical application point of view (Tables 1 and 2, already published earlier). An attempt has also been made to identify the intermediate products formed during the photo-oxidation process through GC/MS analysis technique, which could be useful source of information on the degradation pathways.

We have chosen few selected pesticide derivatives for our study, which have been used extensively in the agricultural field for better quality and quantity of crops. They have a wide range of applications, such as contact, systemic and fumigant insecticides, fungicides, herbicides, etc. For example, the compound chlorotoluron is a selective urea derivative, which is used as herbicide throughout the world acting by inhibition of photosynthesis to regulate the plant growth. It is used for pre- and post-emergence control of annual grass, wild oats, annual meadow grass and many broad leaf weeds in winter wheat, spring and winter barley and winter rye phenoxyacetic acid is used as fungicide. It is also used as an intermediate for the synthesis of dyes, drugs and pesticides. 4-Chlorophenoxyacetic acid is used in the food industry as a plant growth regulator to restrict root growth during seed germination. The amine salts of 2,4,5-trichlorophenoxyacetic acid are extensively used for the control of dicotyledonous weeds in cereal crops. It has been used on wheat, barley, oats, rye, rice, maize and sorghum to kill weeds. Few selected organic pollutants studied include maleic hydrazide [123-33-1] (**1**) [18], propham [122-42-9] (**2**) [19], tebuthiuron [34014-18-1] (**3**) [19], propachlor [1918-16-7] (**4**) [19], chlortoluron [15545-48-9] (**5**) [17], thiram [137-26-8] (**6**) [12], phenoxyacetic acid [122-59-8] (**7**) [20], 2,4,5-trichlorophenoxy acetic acid [93-76-5] (**8**) [20], 4-chlorophenoxy acetic acid [122-88-3] (**9**) [21], uracil [66-22-8] (**10**) [21], 5-bromouracil [51-20-7] (**11**) [21] and bromothymol blue [76-59-5] (**12**) [22] are shown in Charts 1 and 2.

2. Experimental procedures

2.1. Materials

Analytical and laboratory grade compounds mentioned in this review were obtained from different sources and used as such without any further purification. Double distilled water was employed in these studies to make a solution for the irradiation experiments. The photocatalyst, titanium dioxide Degussa P25 (Degussa AG) was used in most of the experiments. Other catalyst powders, namely, Hombikat UV100 (Sachtleben Chemie GmbH) and PC500 (Millennium Inorganic Chemicals), were used for comparative studies. Degussa P25 contains 75% anatase and 25% rutile with a specific BET-surface area of 50 $m^2\ g^{-1}$ and a primary particle size of 20 nm [23]. Hombikat UV100 consists of 100% pure anatase with a specific BET-surface area of 250 $m^2\ g^{-1}$ and a primary particle size of 5 nm [24]. The photocatalyst PC500 has a BET-surface area of 287 $m^2\ g^{-1}$ with 100% anatase and

Table 1

Parameters	Mineralization rate ($mol\ L^{-1}\ min^{-1} \times 10^{-3}$)	Degradation rate ($mol\ L^{-1}\ min^{-1} \times 10^{-3}$)
Tebuthiuron		
Type of photocatalyst		
P25	0.005	0.012
UV100	0.003	0.004
PC500	0.001	0.002
pH		
3.5	0.004	0.0095
5.3	0.005	0.012
7.0	0.006	0.0125
9.0	0.0062	0.013
11.0	0.009	0.018
Substrate concentration (mM)		
0.25	0.004	0.009
0.50	0.005	0.012
0.75	0.0055	0.013
1.0	0.0063	0.014
1.5	0.005	0.011
Catalyst concentration ($g\ L^{-1}$)		
0.5	0.004	0.0085
1.0	0.005	0.012
2.0	0.006	0.014
5.0	0.009	0.0185
7.5	0.009	0.018
Electron acceptors		
P25	0.005	0.012
P25/H_2O_2	0.0062	0.014
P25/$KBrO_3$	0.014	–
P25/$(NH_4)_2S_2O_8$	0.0165	–

Parameters	Mineralization rate ($mol\ L^{-1}\ min^{-1} \times 10^{-3}$)	Degradation rate ($mol\ L^{-1}\ min^{-1} \times 10^{-3}$)
Propachlor		
Type of photocatalyst		
P25	0.020	0.025
UV100	0.0012	0.0016
PC500	0.0.0018	0.0025
pH		
3.0	0.022	0.026
5.0	0.020	0.025
7.0	0.016	0.023
9.0	0.0145	0.021
11.0	0.0100	0.016
Substrate concentration (mM)		
0.2	0.011	0.015
0.4	0.016	0.018
0.6	0.020	0.025
0.8	0.021	0.026
1.35	0.023	0.029
Catalyst concentration ($g\ L^{-1}$)		
0.5	0.0156	0.023
1.0	0.020	0.025
2.0	0.022	0.026
5.0	0.026	0.030
7.0	0.028	0.031
Electron acceptors		
P25	–	0.025
P25/H_2O_2	–	0.028
P25/$KBrO_3$	–	1.0.006
P25/$(NH_4)_2S_2O_8$	–	0.019

Table 1 (*Continued*)

Parameters	Mineralization rate (min^{-1})	Degradation rate ($mol\ L^{-1}\ min^{-1} \times 10^{-5}$)
Chlortoluron		
Type of photocatalyst		
P25	0.190	1.299
UV100	0.171	0.389
PC500	0.109	0.188
pH		
3.0	0.225	1.585
5.4	0.190	1.299
7.3	0.143	1.221
9.1	0.130	1.132
Substrate concentration (mM)		
0.15	0.121	0.946
0.25	0.190	1.299
0.35	0.201	1.416
0.45	0.211	1.555
Catalyst concentration ($g\ L^{-1}$)		
0.5	0.169	0.676
1.0	0.190	1.299
2.0	0.202	1.377
3.0	0.211	1.472
Electron acceptors		
P25	0.190	1.299
P25/H_2O_2	0.232	1.333
P25/$KBrO_3$	0.204	1.642
P25/$K_2S_2O_8$	0.213	1.414

Parameters	Mineralization rate	Degradation rate ($mol\ L^{-1}\ min^{-1} \times 10^{-3}$)
Thiram		
Type of photocatalyst		
P25	–	0.043
UV100	–	0.034
PC500	–	0.035
TTP	–	0.011
pH		
4.0	–	0.076
6.3	–	0.047
8.4	–	0.043
9.8	–	0.042
Substrate concentration (mM)		
0.25	–	0.027
0.40	–	0.042
0.50	–	0.043
0.75	–	0.055
Catalyst concentration ($g\ L^{-1}$)		
0.5	–	0.042
1.0	–	0.043
2.0	–	0.046
3.0	–	0.054
5.0	–	0.058
Electron acceptors		
P25	–	0.043
P25/H_2O_2 (10 mM)	–	0.128
P25/$KBrO_3$ (3 mM)	–	0.237
P25/$(NH_4)_2S_2O_8$ (3 mM)	–	0.154

Parameters	Mineralization rate ($mol\ L^{-1}\ min^{-1} \times 10^{-3}$)	Degradation rate (min^{-1})
Phenoxyacetic acid		

Table 1 (*Continued*)

Parameters	Mineralization rate ($mol\ L^{-1}\ min^{-1} \times 10^{-3}$)	Degradation rate (min^{-1})
Type of photocatalyst		
P25	0.0152	0.0111
UV100	0.0136	0.0087
PC500	0.0088	0.0054
pH		
3.0	0.0152	0.0111
5.0	0.0182	0.0102
7.0	0.0145	0.0072
9.0	0.012	0.0004
Substrate concentration (mM)		
0.25	0.006	0.0059
0.40	0.009	0.087
0.50	0.0152	0.0111
0.75	0.0315	0.0179
Catalyst concentration ($g\ L^{-1}$)		
0.25	0.0114	0.0091
0.50	0.0120	0.0103
1.00	0.0152	0.0111
2.00	0.0140	0.0106
Electron acceptors		
P25	0.0152	0.0111
P25/H_2O_2 (3 mM)	0.0159	0.0131
P25/$KBrO_3$ (3 mM)	0.0293	0.0293

Parameters	Mineralization rate ($mol\ L^{-1}\ min^{-1} \times 10^{-3}$)	Degradation rate (min^{-1})
(2,4,5-Trichlorophenoxy) acetic acid		
Type of photocatalyst		
P25	0.025	0.0255
UV100	0.0057	0.0056
PC500	0.008	0.0085
pH		
3.0	0.025	0.0255
5.0	0.0182	0.0236
7.0	0.0145	0.0199
9.0	0.0126	0.0128
11.0	0.005	0.01
Substrate concentration (mM)		
0.25	0.0192	0.0214
0.50	0.025	0.0255
0.75	0.0265	0.0280
1.0	0.03	0.0311
Catalyst concentration ($g\ L^{-1}$)		
0.5	0.0134	0.0145
1.0	0.025	0.0255
3.00	0.0291	0.0308
5.00	0.024	0.0289
Electron acceptors		
P25	0.025	0.0255
P25/H_2O_2 (3 mM)	0.0432	0.0496
P25/$KBrO_3$ (3 mM)	0.0523	0.0424

Parameters	Mineralization rate ($mol\ L^{-1}\ min^{-1} \times 10^{-3}$)	Degradation rate ($mol\ L^{-1}\ min^{-1} \times 10^{-3}$)
Bromothymol Blue		
Type of photocatalyst		
P25	0.003500	0.010000
UV100	0.002600	0.009000
PC500	0.001100	0.008000
pH		
4.3	0.002400	0.01000
6.8	0.003500	0.010000
8.1	0.003200	0.009800
10.3	0.002900	0.009000
Substrate concentration (mM)		
0.125	0.00210	0.00800
0.25	0.003500	0.010000
0.35	0.003600	0.009900
0.50	0.002200	0.005000
Catalyst concentration ($g\ L^{-1}$)		
0.5	0.000860	0.00400
1.0	0.003500	0.010000
2.00	0.004900	0.012000
3.00	0.007300	0.013000

primary particle size of 5–10 nm [25]. Other reagent grade chemicals used in this study, such as sodium hydroxide, nitric acid, hydrogen peroxide, potassium persulphate, ammonium persulphate and potassium bromate were obtained from Merck.

2.2. Methods

Stock solutions of the compounds (Charts 1 and 2) with desired concentration were prepared in double distilled water. An immersion well photochemical reactor made of Pyrex glass equipped with a magnetic stirring bar, water-circulating jacket and an opening for supply of air bubbling was used.

For irradiation experiments, the solution (250 mL) of the compounds (Charts 1 and 2) with desired concentration was taken into the photoreactor and required amount of photocatalyst was added and the solution was stirred and bubbled with oxygen for at least 15 min in the dark to allow equilibration of the system so that the loss of compound due to adsorption can be taken into account. The zero time reading was obtained from a blank solution kept in the dark but otherwise treated similarly to the irradiated solution. The suspensions were continuously purged with molecular oxygen throughout each experiment. Irradiations were carried out using a 125 W medium pressure mercury lamp (Philips). The light intensity was measured using UV-light intensity detector (Lutron UV-340) and was found to be 4.86 mW cm^{-2}. IR radiation and short-wavelength UV radiation were eliminated by a water-circulating pyrex jacket. Samples (10 mL) were collected before and at regular intervals during the irradiation and centrifuged before analysis. The pH of the reaction mixture was adjusted by adding dilute aqueous solution of NaOH or HNO_3.

For the characterization of intermediate products, aqueous solution (250 mL) of the pollutants containing TiO_2 (P25) was taken in a photochemical reactor made of Duran glass with a plain quartz window (through which the parallel light beam is entering) equipped with a magnetic stirring bar, a water-circulating jacket and opening for electrodes and gas supplies. Irradiations were carried out using a high-pressure mercury lamp (Osram HBO 450 W). The light intensity was found to be

Table 2

Parameters	Uracil		5-Bromouracil	
	Degradation rate (M min^{-1})	Mineralization rate (M min^{-1})	Degradation rate (M min^{-1})	Mineralization rate (M min^{-1})
Type of photocatalyst (1 g L^{-1})				
P25	0.59	0.0083	0.011	0.0028
UV100	0.013	0.0033	0.0098	0.0026
PC500	0.018	0.0046	0.008	0.0023
TTP	0.0032	0.0010	0.0054	0.00037
pH				
3	0.043	0.0056	0.0068	0.0013
5	0.059	0.0083	0.011	0.0028
7	0.061	0.0085	0.019	0.0036
9	0.08	0.0089	0.023	0.0049
Substrate concentration (mM)				
0.25	0.04	0.0071	–	–
0.5	0.059	0.0083	0.010	0.0017
0.75	0.072	0.0103	0.010	0.0027
1.0	0.078	0.0108	0.011	0.0028
1.5	–	–	0.012	0.0029
Catalyst concentration (g L^{-1})				
0.25	0.038	0.0054	–	–
0.5	0.049	0.0069	0.0097	0.0021
1.0	0.059	0.0083	0.011	0.0028
2.0	0.137	0.0116	0.013	0.0032
3.0	–	–	0.019	0.0050

20 mW cm^{-2}. A 10 cm water filter eliminated IR radiation and short-wavelength UV radiation. A 320 nm cut-off filter was used to avoid any direct excitation of the compound under investigation. Samples were collected at different time intervals during the irradiation, centrifuged to remove TiO_2 and extracted with methylene chloride, and subsequently dried over anhydrous sodium sulphate, which was analysed by GC/MS.

2.3. Analysis

The degradation of pollutants and its intermediate products was followed by measuring the change in absorption intensity at their λ_{max} using Shimadzu UV-Vis Spectrophotometer (Model 1601). The mineralization was monitored by measuring the total organic carbon (TOC) content with a Shimadzu TOC 5000A Analyzer by directly injecting the aqueous solution after centrifugation.

For GC/MS analysis, Shimadzu Gas Chromatograph and Mass Spectrometer (GCMS-QP 5050) equipped with a 25 m CP SIL 19 CB ($d = 0.25$ mm) capillary column, operating temperature programmed (220 °C for 40 min at the rate of 10 °C min^{-1}) in split less mode injection volume (1.0 μL), with helium as a carrier gas was used.

3. Results and discussion

3.1. Photocatalysis of TiO_2 suspensions containing organic pollutants

Irradiation of an aqueous solution of the model compounds in the presence of TiO_2 (Degussa P25, 1 g L^{-1}), by the ''pyrex'' filtered output of 125 W medium pressure mercury lamp, led to decrease in absorption intensity and depletion in TOC content as a function of time. As a representative example Fig. 1 shows the change in absorption intensity and depletion in TOC content as a function of irradiation time for the photocatalytic degradation of propham (**2**) in the absence and presence of the photocatalyst. Both the decomposition and mineralization curves can be fitted reasonably well by an exponential decay curve suggesting first order kinetics. For each experiment, the rate constant was calculated from the plot of natural logarithm of TOC and pollutant concentration as a function of irradiation time. The degradation rate for the mineralization (depletion of TOC content versus irradiation time) and decomposition (decrease in absorption intensity versus irradiation time) was calculated using formula given below:

$$\frac{-\mathrm{d}[\mathrm{TOC}]}{\mathrm{d}t} = kc^n \tag{11}$$

$$\frac{-\mathrm{d}[\mathrm{A}]}{\mathrm{d}t} = kc^n \tag{12}$$

TOC is the total organic carbon in millimoles of organic carbon, A the absorbance, k the rate constant, c the concentration of the pollutant in millimoles and n is the order of reaction.

Control experiments were carried out in all cases, employing unirradiated blank solutions. No observable loss of the compound takes place when the irradiation was carried out in the absence of TiO_2. The zero irradiation time reading was obtained from blank solutions kept in the dark, but otherwise treated similarly to the irradiated solutions.

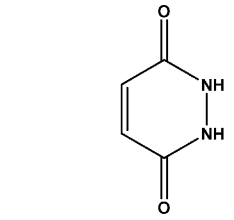

Maleic hydrazide
(1)
1,2-Dihydro-pyridazine-3,6-dione
$C_4H_4N_2O_2$

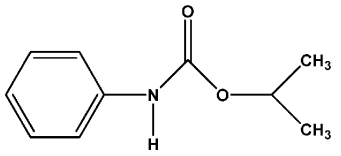

Propham
(2)
Phenyl-carbamic acid isopropyl ester
$C_{10}H_{13}NO_2$

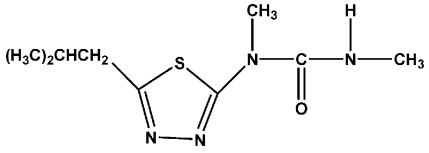

Tebuthiuron
(3)
1-(5-Isobutyl-[1,3,4]thiadiazol-2-yl)-1,3-dimethyl-urea
$C_9H_{16}N_4OS$

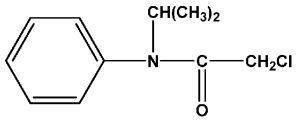

Propachlor
(4)
2-Chloro-*N*-isopropyl-*N*-phenyl-acetamide
$C_{11}H_{14}ClNO$

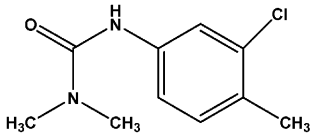

Chlorotoluron
(5)
3-(3-Chloro-4-methyl-phenyl)-1,1-dimethyl-urea
$C_{10}H_{13}ClN_2O$

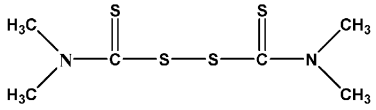

Thiram
(6)
$C_6H_{12}N_2S_4$

Chart 1.

Blank experiments were carried out by irradiating the aqueous solution of the model compounds (Charts 1 and 2) in the absence of TiO_2, where no observable loss of the compound was observed. The zero irradiation time reading was obtained from blank solution kept in the dark in the presence of TiO_2, but otherwise treated similarly to the irradiated solutions. The degradation rate for the decomposition of the compound for the first order reaction was calculated in terms of moles per liter per minute.

3.2. Comparison of different TiO_2 photocatalysts

We have tested the photocatalytic activity of three different commercially available TiO_2 powders (namely, Degussa P25, Hombikat UV100 and Millennium Inorganic PC500) on the degradation kinetics of different model compounds, under investigation. As a representative example, the degradation rate obtained for the decomposition and for the mineralization of propham (**2**) in the presence of different types of TiO_2 powders (1 g L^{-1}) is shown in Fig. 2(a). The photonic efficiency for the decomposition and mineralization of benzidine in the presence of different types of TiO_2 powders is shown in Fig. 2(b). It has been observed that the degradation of the model compound under investigation proceeds much more rapidly in the presence of Degussa P25 as compared with other TiO_2 samples. But in some cases UV100 was found to be better as shown in Fig. 2(b).

The reason for the better photocatalytic activity of Degussa P25, could be attributed to the fact that P25 being composed of small nano-crystallites of rutile being dispersed within an anatase matrix [26]. The band gap energy of anatase is slightly higher than the rutile. Hence when a light intensity of 4.86 mW cm^{-2} was irradiated on TiO_2 surface, the smaller band gap of rutile "catches" the photons, generating electron–hole pair. The electron transfer from the rutile conduction band to electron traps in anatase phase takes place. Recombination is thus inhibited allowing the hole to move to the surface of the particle and react [26].

In all following experiments, Degussa P25 was used as the photocatalyst, since this material exhibited the highest overall activity for the degradation of the pesticide.

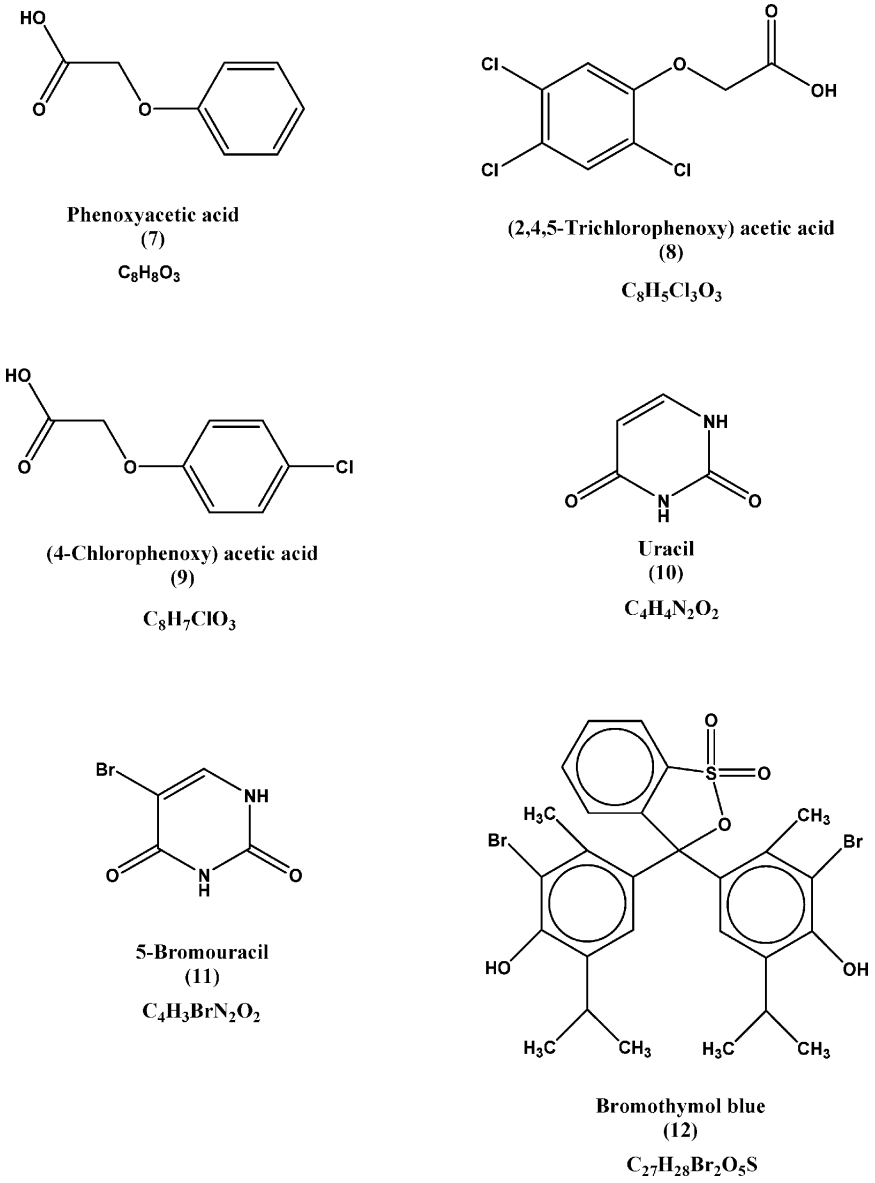

Chart 2.

3.3. Effect of pH

Another important parameter in the photocatalytic reactions taking place on the particulate surfaces is the pH of the solution, since it dictates the surface charge properties of the photocatalyst and size of aggregates it forms. Employing Degussa P25 (1 g L^{-1}) as photocatalyst the decomposition and mineralization of different model compounds in aqueous suspensions was studied in the pH range between 1 and 12. As a representative example Fig. 3(a and b), show the degradation rate for the TOC depletion and for the decomposition of the pesticide derivatives **2** and **3**, respectively, as a function of pH. It is interesting to note that the degradation rate for the TOC depletion and decomposition of propham (**2**) was found to be better at lower pH, which decreases with increase in reaction pH, whereas in the case of tebuthiuron (**3**), the degradation rate increases with the increase in reaction pH.

The interpretation of pH effect on the photocatalytic process is a difficult task because of its multiple role, such as electrostatic interactions between the semiconductor surface, solvent molecules, substrate and charged radicals formed during the reaction process. The ionization state of the surface of the photocatalyst can be protonated and deprotonated under acidic and alkaline conditions, respectively, as shown in following equations:

$$\mathrm{TiOH} + \mathrm{H^+} \rightarrow \mathrm{TiOH_2^+} \quad (13)$$

$$\mathrm{TiOH} + \mathrm{OH^-} \rightarrow \mathrm{TiO^-} + \mathrm{H_2O} \quad (14)$$

The point of zero charge (pzc) of the TiO_2 (Degussa P25) is widely reported at pH $\sim$ 6.25 [27]. Thus, the TiO_2 surface will remain positively charged in acidic medium (pH $<$ 6.25) and negatively charged in alkaline medium (pH $>$ 6.25). The amino and carbonyl groups present in the model pollutant can be protonated and deprotonated depending on the pH of the

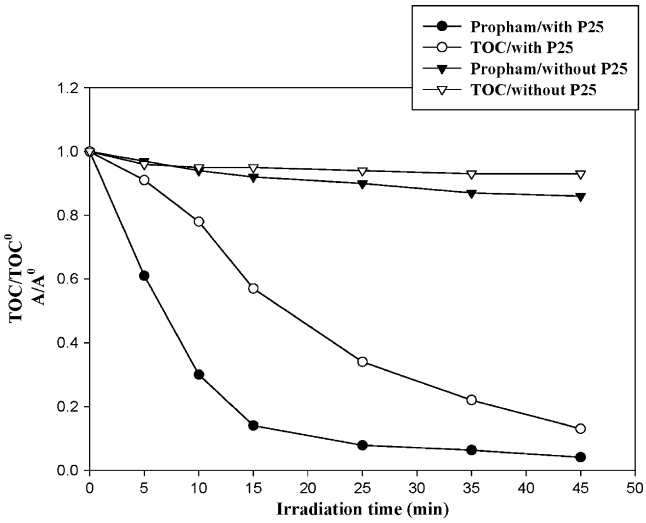

Fig. 1. Depletion in TOC and change in absorption intensity as a function of irradiation time for an aqueous solution of propham (**2**) in the presence and absence of TiO_2. Experimental conditions: substrate concentration (0.5 mM), V = 125 mL, immersion well photoreactor, 125 W medium pressure Hg lamp, TiO_2 (Degussa P25, 1 g L^{-1}), cont. O_2 purging and stirring, irradiation time = 45 min.

reaction mixture. The better degradation rate in acidic pH may be attributed on the basis of the fact that the structural orientation of the molecule is favored for the attack of the reactive species under this condition. The higher efficiency of degradation of tebuthiuron (**3**), in alkaline medium may be attributed to more efficient generation of hydroxyl radicals by TiO_2 with increasing concentration of OH^-. At the alkaline pH values, the hydroxyl radicals have to diffuse away and degrade the compound in the bulk solution.

3.4. Effect of substrate concentration

It is important both from mechanistic and from application point of view to study the dependence of substrate concentration on the photocatalytic reaction rate. Hence, the influence of substrate concentration on the degradation rate of the model compounds as shown in Charts 1 and 2, were studied at different substrate concentrations. As a representative example the degradation rate for the TOC depletion and for the decomposition of compounds **2** and **4** as a function of substrate concentration (0.2–1.3 mM) employing Degussa P25 (1 g L^{-1}) as photocatalyst is shown in Fig. 4(a and b). It is interesting to note that the degradation rate for the propham (**2**) increases with increase in substrate concentration up to certain limit and a further increase in substrate concentration led to decrease the degradation rate whereas in case of propachlor (**4**) the degradation rate was found to increase continuously with increase in substrate concentration. The degradation rate increases with the increase in substrate concentration from 0.25 to 0.75 mM for propham (**2**) and a further increase in the concentration of substrate led to decrease in the degradation rate in presence of P25. The possible explanation for this behavior is that as the concentration of model pollutant increases, more and more molecules of the compound get adsorbed on the surface of the photocatalyst, therefore, the requirement of catalyst surface needed for the degradation also increases. Hence, the generations of relative amounts of $^{\bullet}OH$ and $O_2^{\bullet-}$ on the surface of the catalyst do not increase as the intensity of light, irradiation time and amount of catalyst are constant. Consequently, the degradation efficiency of the model pollutant decreases as the concentration increases. However, in case of propachlor (**4**), the degradation rate was found to increase continuously from 0.25 to 1.35 mM.

As oxidation proceeds, less and less of the surface of the TiO_2 particle is covered as the pollutant is decomposed. Evidently, at total decomposition the rate of degradation is zero and a decreased photocatalytic rate is to be expected with increasing irradiation time. It has been agreed with minor variation that the expression for the rate of photomineralization of organic substrates with irradiated TiO_2

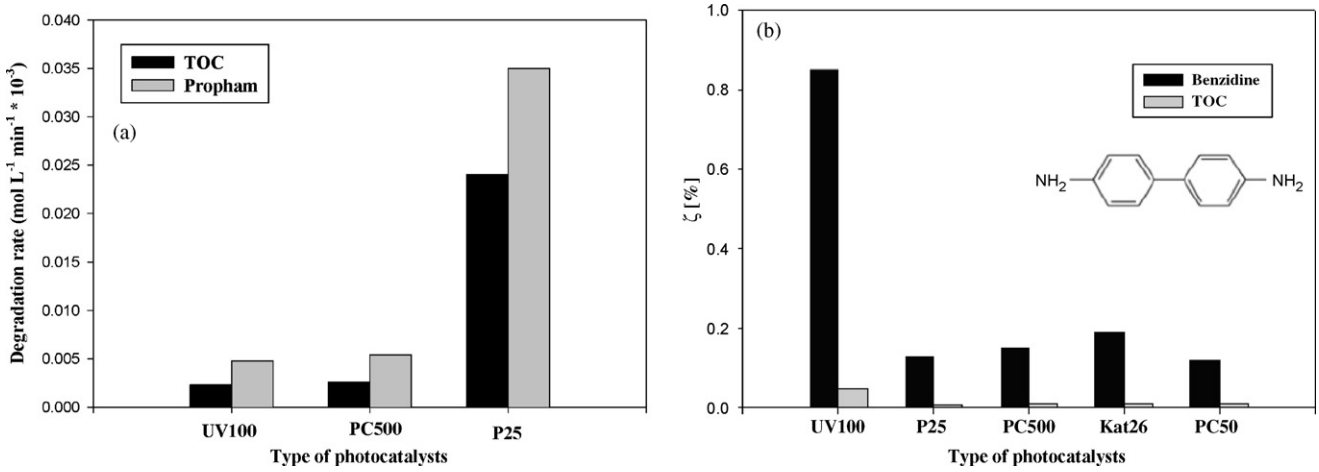

Fig. 2. (a) Comparison of degradation rate for the mineralization and decomposition of propham (**2**) in the presence of different photocatalysts. Experimental conditions: substrate concentration (0.5 mM), V = 125 mL, Degussa P25 (1 g L^{-1}), Sachtleben Hombikat UV100 (1 g L^{-1}), PC500 (1 g L^{-1}), immersion well photoreactor, 125 W medium pressure Hg lamp, cont. O_2 purging and stirring, irradiation time = 45 min. (b) Comparison of degradation rate for the mineralization and decomposition of benzidine in the presence of different photocatalysts. Experimental conditions: substrate concentration (0.5 mM), V = 250 mL, Degussa P25 (1 g L^{-1}), Sachtleben Hombikat UV100 (1 g L^{-1}), PC500 (1 g L^{-1}), Kat 26 (1 g L^{-1}), PC50 (1 g L^{-1}) immersion well photoreactor, 125 W medium pressure Hg lamp, cont. O_2 purging and stirring.

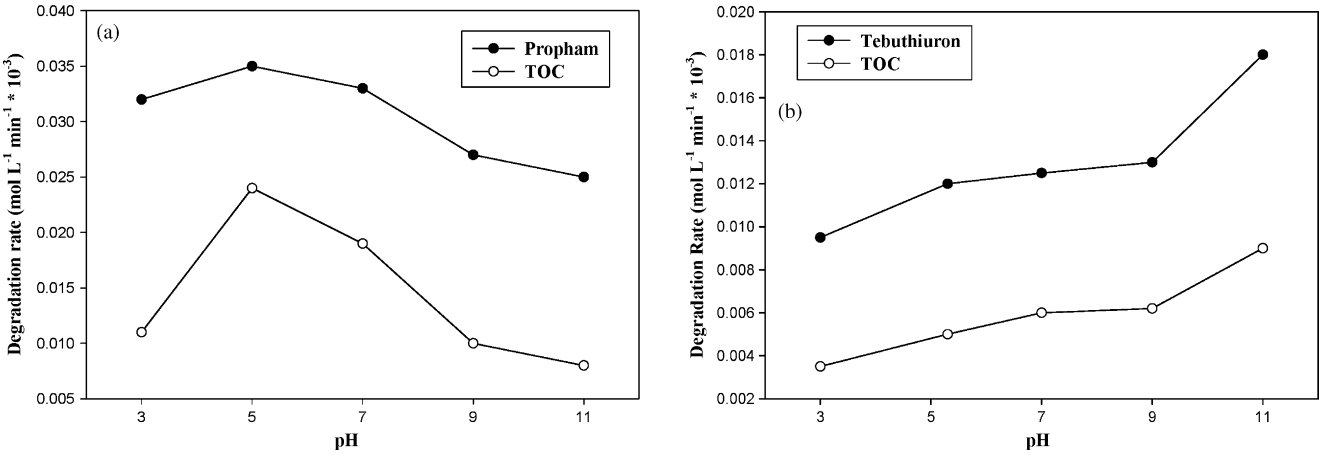

Fig. 3. (a) Influence of pH on the degradation rate for the mineralization and decomposition of propham (**2**) in presence of Degussa P25. Experimental conditions: substrate concentration (0.5 mM), $V = 125$ mL, catalyst concentration (1 g L^{-1}), reaction pH (3, 5, 7, 9 and 11), immersion well photoreactor, 125 W medium pressure Hg lamp, cont. O_2 purging and stirring, irradiation time = 45 min. (b) Influence of pH on the degradation rate for the mineralization and decomposition of tebuthiuron (**3**) in presence of Degussa P25. Experimental conditions: substrate concentration (0.5 mM), $V = 125$ mL, catalyst concentration (1 g L^{-1}), reaction pH (3, 5, 7, 9 and 11), immersion well photoreactor, 125 W medium pressure Hg lamp, cont. O_2 purging and stirring, irradiation time = 120 min.

follows the Langmuir–Hinshelwood (L–H) law for the four possible situations, i.e. (a) the reaction takes place between two adsorbed substances, (b) the reaction occurs between a radical in solution and an adsorbed substrate molecule, (c) the reaction takes place between a radical linked to the surface and a substrate molecule in solution and (d) the reaction occurs with both the species being in solution [28]. In all cases, the expression for the rate equation is similar to that derived from the L–H model, which has been useful in modeling the process although it is not possible to find out whether the process takes place on the surface, in the solution or at the interface.

Earlier studies [28–31] on the photocatalytic degradation of colorless organic pollutants also indicate that the degradation rate increases with the increase in substrate concentration.

3.5. Effect of catalyst concentration

The influence of the photocatalyst concentration on the degradation for the decomposition and mineralization of various organic pollutants were investigated using different concentrations of TiO_2 powder. As a representative example the effect of photocatalyst concentration on the degradation kinetics of propham (**2**) was investigated employing different concentrations of Degussa P25, varying from 0.5 to 5 g L^{-1}. The degradation rate for the TOC depletion and for the decomposition of the pesticide derivative **2** as function of catalyst loading is shown in Fig. 5. As expected, the degradation rate was found to increase with the increase in catalyst concentration, which is the characteristic of heterogeneous photocatalysis and results are in agreement with

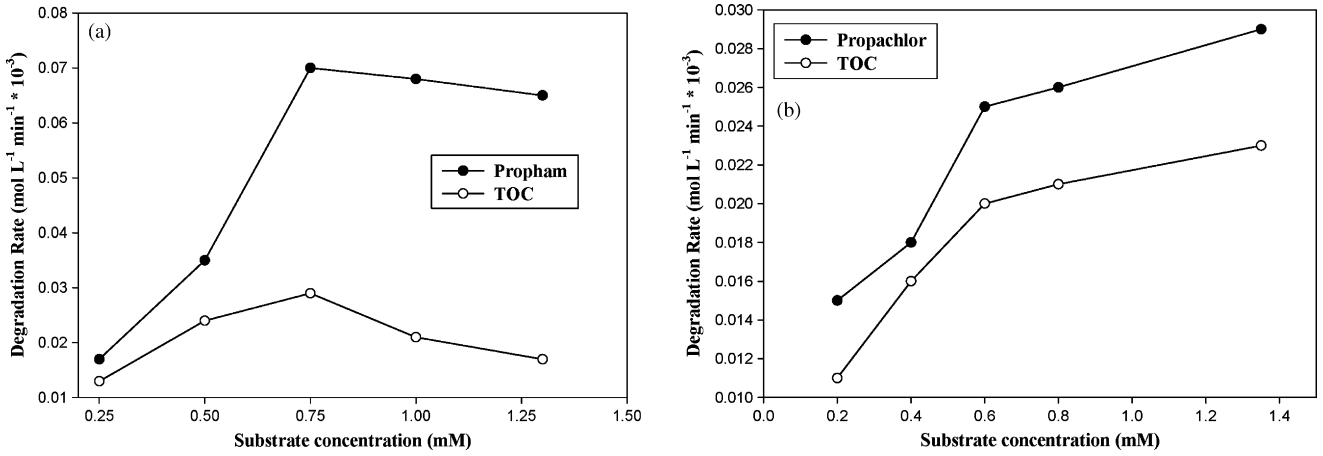

Fig. 4. (a). Influence of substrate concentration on the degradation rate for the mineralization and decomposition of propham (**2**) in presence of Degussa P25. Experimental conditions: substrate concentrations (0.25, 0.5, 0.75, 1 and 1.3 mM), $V = 125$ mL, immersion well photoreactor, 125 W medium pressure Hg lamp, catalyst concentration (1 g L^{-1}), cont. O_2 purging and stirring, irradiation time = 45 min. (b) Influence of substrate concentration on the degradation rate for the mineralization and decomposition of propachlor (**4**) in presence of Degussa P25. Experimental conditions: substrate concentrations (0.2, 0.4, 0.6, 0.8 and 1.35 mM), $V = 125$ mL, immersion well photoreactor, 125 W medium pressure Hg lamp, catalyst concentration (1 g L^{-1}), cont. O_2 purging and stirring, irradiation time = 75 min.

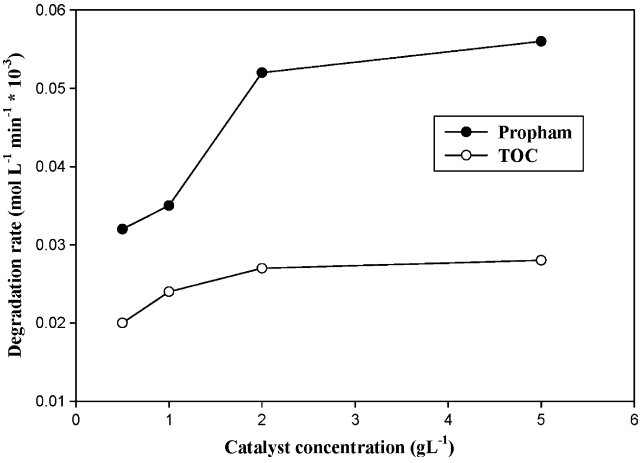

Fig. 5. Influence of catalyst concentration on the degradation rate for the mineralization and decomposition of propham (**2**) in presence of Degussa P25. Experimental conditions: substrate concentration (0.5 mM), $V = 125$ mL, immersion well photoreactor, 125 W medium pressure Hg lamp, catalyst concentration (0.5, 1, 2 and 5 g L^{-1}), cont. O_2 purging and stirring, irradiation time = 45 min.

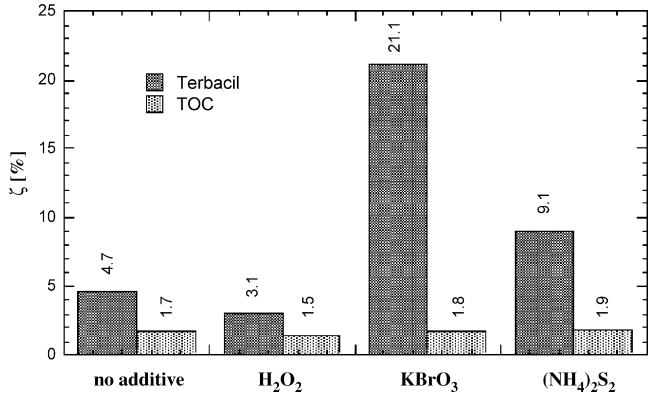

Fig. 6. Photonic efficiencies for the photocatalytic degradation and for the mineralization (TOC) of Terbacil in the presence of different oxidants using pH stat-technique. Experimental conditions: 0.25 mM Terbacil, $V = 250$ mL, pH 5, electron acceptors: H_2O_2 (10 mM), $KBrO_3$ (3 mM) and $(NH_4)_2S_2O_8$ (3 mM), P25 (1 g L^{-1}), cont. O_2 purging and stirring, time = 6 h.

number of studies reported earlier [32,33] and also with other compounds mentioned here.

Whether in static, slurry or dynamic flow reactors the initial reaction rates were found to be directly proportional to catalyst concentration indicating a heterogeneous regime. However, it was observed that above a certain concentration the reaction rate decreases and becomes independent of the catalyst concentration. This limit depends on the geometry and working conditions of the photoreactor and for a definite amount of TiO_2 in which all the particles, i.e. surface exposed are totally illuminated. When the catalyst concentration is very high, after traveling a certain distance on an optical path, turbidity impedes further penetration of light in the reactor. In any given application, this optimum catalyst concentration $[(TiO_2)_{OPT}]$ must be determined, in order to avoid excess catalyst and insure total absorption of efficient photons.

3.6. Effect of electron acceptors

One practical problem in using TiO_2 as a photocatalyst is the undesired electron/hole recombination which, in the absence of proper electron acceptor or donor is extremely efficient and represent the major energy-wasting step thus limiting the achievable quantum yield. One strategy to inhibit electron–hole pair recombination is to add other (irreversible) electron acceptors to the reaction. They could have several different effects, such as (1) to increase the number of trapped electrons and, consequently, avoid recombination, (2) to generate more radicals and other oxidizing species, (3) to increase the oxidation rate of intermediate compounds and (4) to avoid problems caused by low oxygen concentration. In highly toxic wastewater where the degradation of organic pollutants is the major concern the addition of electron acceptors to enhance the degradation rate may often be justified. With this view, we have studied the effect of electron acceptors, such as potassium persulphate, ammonium persulphate, potassium bromate and hydrogen peroxide in the presence of TiO_2 (Degussa P25, 1 g L^{-1}) on the photocatalytic degradation of the model compounds shown in Charts 1 and 2. As a representative example we have studied the effect of electron acceptors, such as ammonium persulphate (3 mM), potassium bromate (3 mM) and hydrogen peroxide (10 mM) in the presence of TiO_2 (Degussa P25, 1 g L^{-1}) on the photocatalytic degradation of the model compound **7** under investigation and the result are depicted in Fig. 6.

Among all the additives, potassium bromate showed a pronounced effect for the decomposition of the compound **7**, while ammonium persulphate shows better mineralization rate as compared to other additives.

The electron acceptors, such as hydrogen peroxide, bromate and persulphate ions are known to generate hydroxyl radicals by the mechanisms shown in Eqs. (15)–(18):

$$BrO_3^- + 2H^+ + e_{cb}^- \rightarrow BrO_2 + H_2O \quad (15)$$

$$BrO_3^- + 6H^+ + 6e_{cb}^- \rightarrow [BrO_2^-, HOBr] \rightarrow Br^- + 3H_2O \quad (16)$$

$$S_2O_8^{2-} + e_{cb}^- \rightarrow SO_4^{2-} + SO_4^- \quad (17)$$

$$SO_4^- + H_2O \rightarrow SO_4^{2-} + OH^\bullet + H^+ \quad (18)$$

The respective one-electron reduction potentials of different species are: $E(O_2/O_2^{\bullet-}) = -155$ mV or -146 mV, $E(H_2O_2/OH^\bullet) = 800$ or 1776 mV, $E(BrO_3^-/BrO_2^\bullet) = 1150$ mV, and $E(S_2O_8^{2-}/SO_4^-) = 1100$ or 2123 mV [34,35]. From the thermodynamic point of view, all employed additives should therefore be more efficient electron acceptors than molecular oxygen.

The effective electron acceptor ability of $KBrO_3$ has been observed in number of studies reported before [33,36]. The reason can be attributed to the number of electrons it reacts as shown in Eq. (16). Another possible explanation might be a change in the reaction mechanism of the photocatalytic degradation. Since the reduction of bromate ions by electrons does not lead directly to the formation of hydroxyl radicals, but

rather to the formation of other reactive radicals or oxidizing agents, e.g. BrO_2^- and HOBr. Linder has proposed a mechanism for the photocatalytic degradation of 4-chlorophenol in the presence of bromate ions considering direct oxidation of the substrate by bromate ions [37]. A similar mechanism might be operative in the model compound **7** under investigation.

The effect of H_2O_2 has been investigated in numerous studies and it was observed that it increases the photodegradation rates of organic pollutants. The enhancement of the degradation rate on addition of H_2O_2 can be rationalized in terms of several reasons. Firstly, it increases the rate by removing the surface-trapped electrons, there by lowering the electron–hole recombination rate and increasing the efficiency of hole utilization for reactions, such as ($OH^- + h^+ \rightarrow OH^\bullet$). Secondly, H_2O_2 may split photolytically to produce hydroxyl radicals directly, as cited in studies of homogeneous photooxidation using UV/($H_2O_2 + O_2$) [38].

During the photocatalytic degradation the free radicals formed serve a dual function. They are not only the strong oxidants but also at the same time their formation and subsequent rapid oxidation reactions inhibit the electron hole pair recombination.

3.7. Intermediate products

3.7.1. Photolysis of TiO_2 suspensions containing propham (2)

Irradiation of an aqueous solution of propham (**2**) in the presence of Degussa P25 (2 g L^{-1}) and analysis of the irradiated mixture at different time intervals through GC/MS analysis showed the formation of several intermediate products. It has been observed that two products appear after 1 h of irradiation at retention times (t_R) 12.95 and 14.81 min, respectively. Both products have identical molecular ion and fragmentation pattern as indicated below,

Compound **14**: 195 (M^+), 153, 135, 109, 81, 59, 43 and 41.

They have been characterized as hydroxyl added product (**14**). The appearance of two products indicate the formation of both *ortho*- and *para*-addition product. A cleavage product, **19** has also been characterized on the basis of molecular ion peak and fragmentation pattern as indicated below,

Compound **19**: 125 (M^+), 111, 98, 84, 83, 70, 69, 56, 43 and 41.

The formation of intermediate products, such as **14** and **19** from propham (**2**) involving electron transfer reactions and reactions with hydroxyl radical and superoxide radical anions formed in photocatalytic system, are shown in Scheme 1, which was published earlier [19]. The model compound **1** upon the transfer of an electron can form the radical anion **13**, which may undergo addition of a hydroxyl radical either at ortho or para position followed by loss of a proton to give the observed product **14**. This compound on further transfer of an electron followed by addition of a hydroxyl group can undergo cleavage reaction to give **15**. This intermediate on subsequent transfer of an electron can undergo addition of a hydroxyl group to give the observed product **19**.

3.7.2. Photolysis of TiO_2 suspensions containing propachlor (4)

Irradiation of an aqueous solution of propachlor (**4**) in the presence of Degussa P25 (2 g L^{-1}) and analysis of the irradiated mixture at different time intervals through GC/MS analysis showed the formation of several intermediate products.

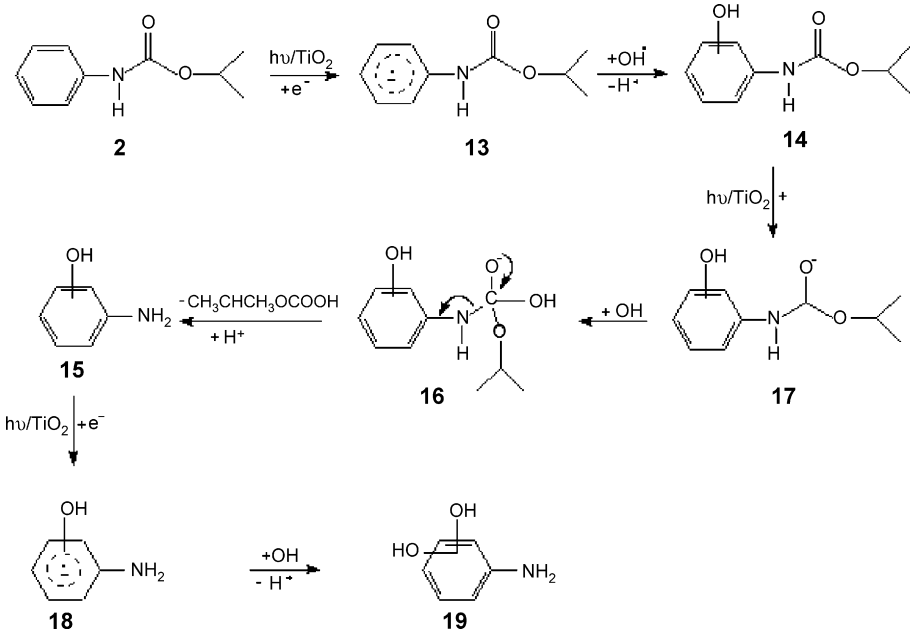

Scheme 1.

The reaction of this model compound also indicates the formation two products appearing at retention times (t_R) 17.48 and 17.86 min, respectively. Both the products showed identical molecular ion and similar fragmentation peaks as observed in the case of propham (**2**). Here, also it is expected that the hydroxyl group undergoes insertion reaction at ortho and para positions of the benzene ring and assigned as **25**. Other products, such as **23**, **26** and **21** appearing at retention times (t_R) 11.26, 12.56 and 23.83 min have been proposed on the basis of molecular ion and mass fragmentation pattern which are indicated below:

Compound **21**: 227 (M^+), 212, 192, 177, 149, 136, 118, 109, 93, 77, 57, 43 and 41.
Compound **23**: 191(M^+), 177, 149, 134, 120, 108, 90, 79, 65, 44, 41 and 40.
Compound **25**: 177 (M^+), 161, 149, 127, 121, 105, 91, 77, 57, 43 and 41.
Compound **26**: 135 (M^+), 120, 107, 91, 77, 57, 44 and 41.

The photocatalytic reaction of this model compound was also studied in the presence of two different TiO_2 samples, such as Hombikat UV100 and Pt/TiO_2. It has been observed that in all three TiO_2 samples similar products were formed. It is interesting to note that the formation of products were faster in the presence of Pt/TiO_2 and it slower in Hombikat UV100.

A plausible mechanism for the formation of the different products, such as **21**, **23**, **25** and **26** from propachlor (**4**) involving similar reactive species, is proposed in Scheme 2, which was already being published [19]. The model compound, **4** on transfer of an electron can form the radical species **20** on removal of chloride ion. The radical species can lead to the observed products **21** and **23**, on abstraction of a hydrogen atom on hydroxyl radical. The product **21**, on further transfer of an electron can form the radical species **24**, which may loose isopropyl to give the observed product **26**. The formation of **25** could be understood in terms of pathways shown in Scheme through electron transfer to give radical anion species **22** followed by addition of hydroxyl radical.

3.7.3. Photolysis of TiO_2 suspensions containing chlortoluron (5)

An aqueous suspension of chlortoluron (**5**, 0.35 mM, 250 mL) in the presence of TiO_2 (Degussa P25, 1.5 g L^{-1}) under constant bubbling of atmospheric oxygen was irradiated for 2 h. The catalyst was removed through centrifugation and irradiated aqueous solution was extracted with methylene

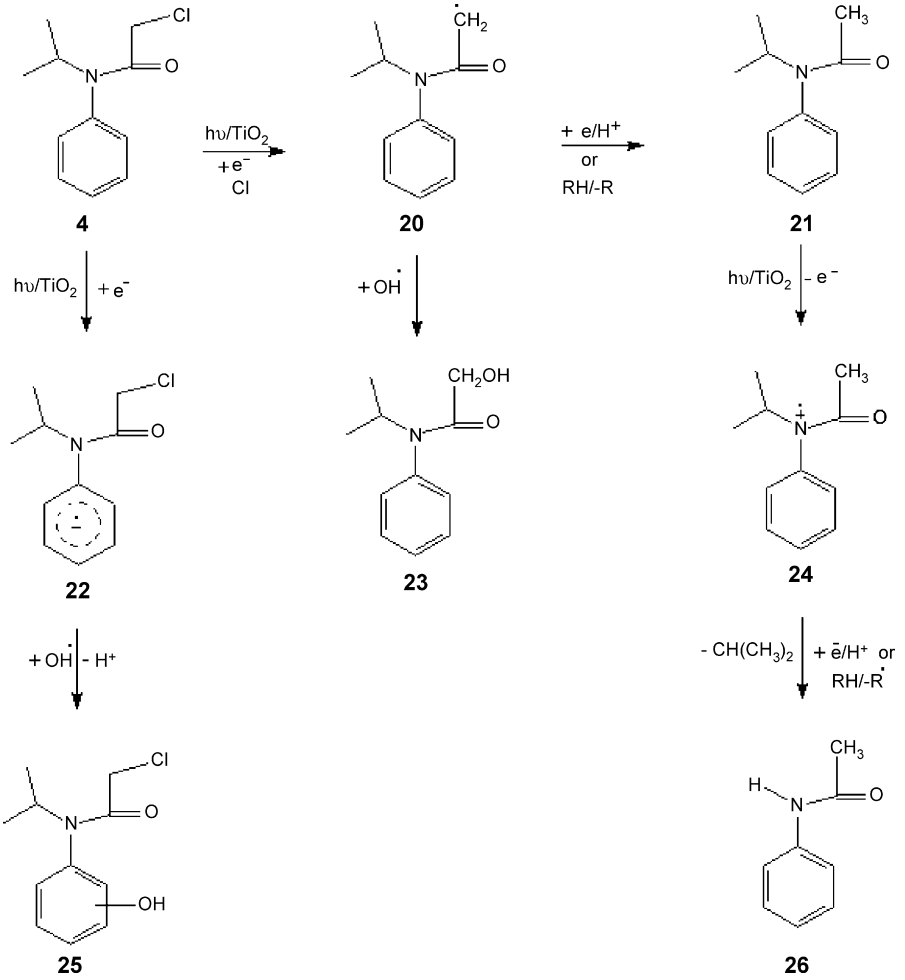

Scheme 2.

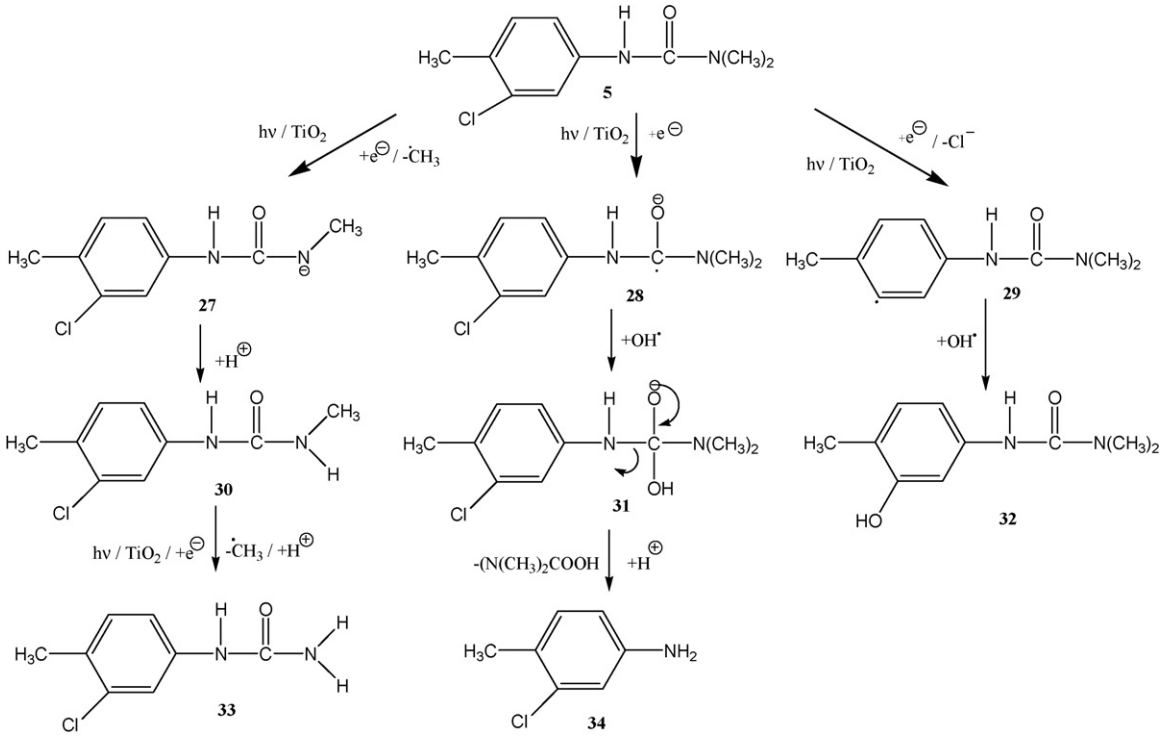

Scheme 3.

chloride, which was dried over anhydrous sodium sulphate. The GC/MS analysis of the organic extract showed the formation of several intermediate product out of which three products, such as 3-(3-hydroxy-4-methylphenyl)-1,1-dimethylurea (**32**) (3-chloro-4-methylphenyl) urea (**33**) and 3-chloro-4-methylphenylamine (**34**) appearing at retention times (t_R) 10.310, 10.255 and 5.520 min, respectively, along with some unchanged starting material (**5**) appearing at (t_R) 5.097 min were identified. It is pertinent to mention here that the model compound **5** did not show the molecular ion peak, instead it showed the peak equivalent to the loss of $N(CH_3)_2$ group. The products were characterized by comparing the molecular ion and mass fragmentation pattern with those reported in the GC/MS NIST library, as indicated below.

Compound **33**: 178 (M^+), 161, 146, 128, 118, 104, 84, 72, 63, 44 and 41
Compound **34**: 135 (M^+), 120, 103, 91, 77, 58, 49 and 41
Compound **32**: 164 (M^+), 148, 135, 119, 106, 91, 72, 65, 44 and 39
Compound **5**: 161 (M^+, $-N(CH_3)_2$), 146, 128, 118, 103, 91, 77, 58, 51 and 41.

When the reaction of the model compound **5** was carried out in the presence of Hombikat UV100 (100% anatase with BET-surface area of 250 $m^2\ g^{-1}$), a difference in the yield of the above products were observed with that of the Degussa P25 (75% anatase and 25% rutile with BET-surface area of 50 $m^2\ g^{-1}$).

A possible mechanism for the formation of products **32**, **33** and **34** from chlortoluron (**5**) involving electron transfer reaction and reaction with hydroxyl radicals could be understood in terms of pathways shown in Scheme 3, which was already being published [17]. The model compound **5**, upon the transfer of an electron followed by the loss of methyl radical and abstraction of a proton to give species **30**. This species on subsequent similar reaction can give the observed product **33**. The observed product **34** from **5** may be arising through the transfer of an electron to give radical anionic species **28**, which

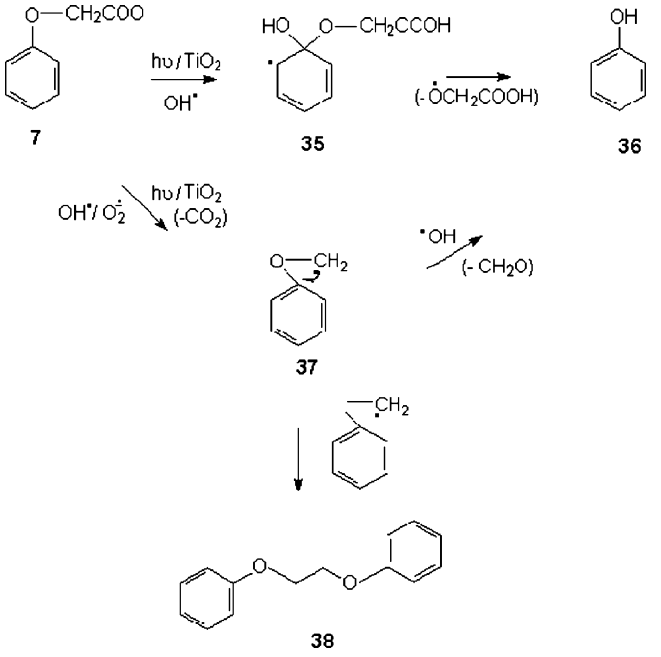

Scheme 4.

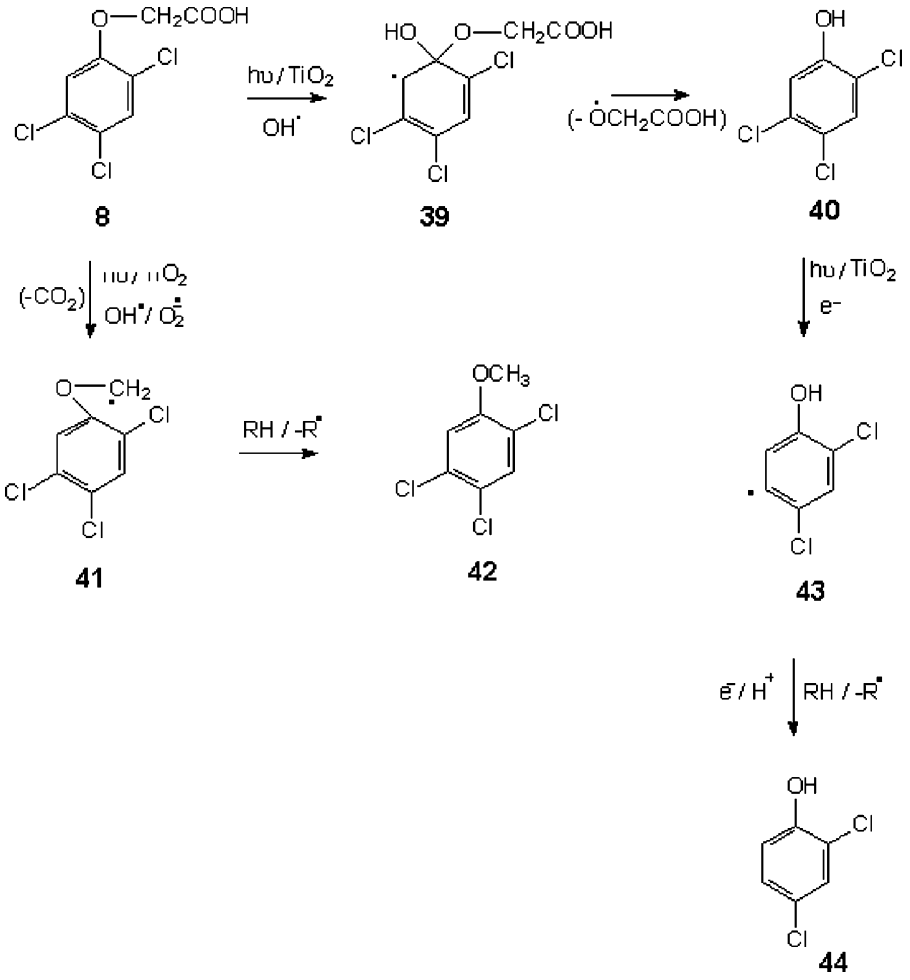

Scheme 5.

may undergo addition of a hydroxyl radical to give **31**. This species may lose $N(CH_3)_2COOH$ followed by abstraction of a proton to give the observed product **34** as shown in the Scheme 3. The product **32** could be formed upon the transfer of an electron followed by the loss of chloride ion with subsequent addition of hydroxyl radical. The analysis of the intermediate products formed during the photodegradation process could be a useful source of information on the degradation pathways.

3.7.4. Photolysis of TiO_2 suspensions containing phenoxyacetic acid (7)

An aqueous suspension of phenoxyacetic acid (**7**, 1 mM, 250 mL) in the presence of Degussa P25 (1 g L^{-1}) was irradiated for 1 h. The catalyst was removed by filtration and the solution was extracted with chloroform, which was dried over anhydrous sodium sulfate. The removal of the solvent under reduced pressure gave a residual mass, which was analysed by GC–MS analysis. The analysis showed the formation of two intermediate products phenol (**36**) and 1,2-diphenoxyethane (**38**) appearing at retention time (t_R) 2.92 and 9.84 min, respectively. These products were identified by comparing its molecular ion and mass fragmentation peaks with those reported in the NIST library. A plausible mechanism for the formation of these products involving reactions with hydroxyl radical and superxoide radical anion formed in the photoctalytic process is shown in Scheme 4, which was already being published [20]. The model compound undergoes addition of a hydroxyl radical leading to the formation of a radical species **35**, which may undergo loss of ($^{\bullet}OCH_2COOH$) to give the observed product phenol (**36**). Alternatively, the model compound **7** on addition of hydroxyl radical followed by loss of CO_2 may lead to the formation of the radical species **37**. This species can either lose formaldehyde molecule followed by addition of hydroxyl radical led to the formation of phenol or can combine with another radical species leading to the formation of the 1,2-diphenoxyethane (**38**).

3.7.5. Photolysis of TiO_2 suspensions containing 2,4,5-trichlorophenoxy acetic acid (8)

The GC–MS analysis of the irradiated samples of 2,4,5-trichlorophenoxy acetic acid (**8**) in the presence of Degussa P25 showed the formation of three intermediate products, namely, 2,4,5-trichlorophenol **(40)**, 2,4-dichlorophenol **(44)** and 1,2,4-trichloro-5-methoxy benzene (**42**) appearing at retention times 4.11, 6.3 and 12.86 min, respectively, and were identified by comparing their molecular ion and mass fragmentation peaks with those reported in the NIST library.

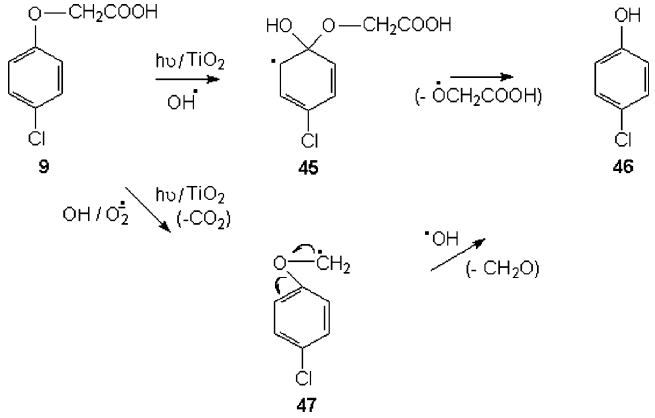

Scheme 6.

The model compound **8** on addition of a hydroxyl radical can lead to the formation of a radical species **39**, which may undergo loss of ($^{\bullet}OCH_2COOH$) group to give the observed product 2,4,5-trichlorophenol (**40**). Alternatively, the model compound **8** upon the transfer of an electron followed by loss of CO_2 may lead to the formation of the radical species **41**. This species abstracts a hydrogen atom to form the observed product 1,2,4-trichloro-5-methoxy benzene (**42**). The product, **40** on further transfer of an electron may undergo loss of chlorine atom followed hydrogen atom abstraction giving 2,4-dichlorophenol (**44**) as shown in Scheme 5, which was already being published [20].

*3.7.6. Photolysis of TiO_2 suspensions containing 4-chlorophenoxy acetic acid (**9**)*

An attempt was made to identify the intermediate products formed in the photocatalytic degradation of the compound 4-chlorophenoxy acetic acid (**9**), in aqueous suspensions of titanium dioxide through GC–MS analysis.

Irradiation of an aqueous suspension of 4-chlorophenoxyacetic acid (**9**, 0.5 mM, 250 mL) in the presence of Degussa P25 (1 g L^{-1}) for 1 h followed by workup by the reaction mixture through removal of catalyst, extraction of aqueous suspension in chloroform. Removal of the solvent under reduced pressure, gave a residual mass, which was analysed by GC–MS. The analysis showed the formation of one intermediate product, 4-chlorophenol (**46**) appearing at retention time (t_R) 6.6 min. The product was identified by comparing its molecular ion and fragment ion peak with those reported in the NIST library. A plausible mechanism for the formation of product, **46** involving reactions with hydroxyl radicals formed in the photocatalytic process is shown in Scheme 6, which was already being published [21]. The model compound, 4-CPA undergoes addition of a hydroxyl radical formed in the photocatalytic process leading to the formation of a radical species **45** as an intermediate, which may undergo loss of ($^{\bullet}OCH_2COOH$) group to give the observed product 4-chlorophenol (**46**). Alternatively, the model compound 4-CPA (**9**) on addition of hydroxyl radical followed by loss of CO_2 may lead to the formation of the intermediate radical species **47**, which upon loss of formaldehyde molecule followed by addition of hydroxyl radical led to the formation of the observed product 4-chlorophenol (**46**).

4. Conclusion

The results of this study clearly indicate that TiO_2 can efficiently catalyse the photodegradation and photomineralization of the pollutants in the presence of light and oxygen. The photocatalyst Degussa P25 was found to be more efficient as compare to other photocatalyst TiO_2 powders. The change in the concentration of the substrate and of the catalyst could influence the kinetics of the processes described by the Langmuir–Hinshelwood model (the reaction order, the adsorption of the model compounds, the change in the order, etc.). The addition of electron acceptor enhanced the degradation rate of the pollutants. The observations of these investigations clearly demonstrate the importance of choosing the optimum degradation parameters to obtain high degradation rate, which is essential for any practical application of photocatalytic oxidation processes. The intermediate products formed during the process are also a useful source of information for the degradation pathways. The results also indicate that degradation rates could be influenced not only by the different parameters, such as type of photocatalyst, catalyst concentration, substrate concentration, pH and additives and their concentration but also by the model pollutants. The best degradation condition depends strongly on the kind of pollutant.

References

[1] Z.Z. Cohen, C. Eiden, M.N. Lober, Evalution of pesticide in ground water, in: W.Y. Gerner (Ed.), ACS Symp. Ser. 315, American Chemical Society, Washington, DC, 1986, pp. 170–196.
[2] L. Muszkat, D. Raucher, M. Mogaritz, D. Ronen, in: U. Zoller (Ed.), Groundwater Contamination and Control, Marcel Dekker, 1994, pp. 257–271.
[3] R.M. Dowd, M.P. Anderson, M.L. Johnson, in: Proceedings of the Second National Outdoor Action Conference on Aquifer Restoration, Groundwater Monitoring Geophysical Methods, National Water Well Association, Dublin, OH, 1988, pp. 1365–1379.
[4] J. Weber, V.C. Stickney, Water Res. 27 (1993) 63.
[5] C. Ràfols, D. Barceló, J. Chromatogr. A 777 (1997) 177.
[6] A. Houas, H. Lachheb, M. Ksibi, E. Elaloui, C. Guillard, J.M. Hermann, Appl. Catal. B: Environ. 31 (2001) 145.
[7] H. Zollinger (Ed.), Color Chemistry: Synthesis, Properties and Applications of Organic Dyes and Pigments, second revised ed., VCH, 1991.
[8] A. Bianco-Prevot, C. Baiocchi, M.C. Brussino, E. Pramauro, P. Savarino, V. Augugliaro, G. Marci, L. Palmisano, Environ. Sci. Technol. 35 (2001) 971.
[9] D.M. Blake, Bibliography of Work on the Photocatalytic Removal of Hazardous Compounds from Water and Air, Cole Boulevard Golden, Colorado, National Renewal Energy Laboratory, 2001.
[10] A. Aguedach, S. Brosillon, J. Morvan, E.K. Lhadi, Appl. Catal. B: Environ. 57 (2005) 55.
[11] K. Pirkanniemi, M. Sillanpää, Chemosphere 48 (2002) 1047.
[12] M.M. Haque, M. Muneer, Ind. J. Chem. Technol. 2 (2005) 68.
[13] M.M. Haque, M. Muneer, J. Environ. Manage. 69 (2003) 169.
[14] K. Macounova, J. Urban, H. Krysova, J. Krysa, J. Jirkovsky, J. Ludvik, J. Photochem. Photobiol. A: Chem. 140 (2001) 93.
[15] H. Fang, D.D. Sun, M. Wu, W. Phay, J.H. Tay, Water Sci. Technol. 51 (2005) 373.

[16] J. Lee, W. Choi, J. Yoon, Environ. Sci. Technol. 39 (2005) 6800.
[17] M.M. Haque, M. Muneer, D.W. Bahnemann, Environ. Sci. Technol. 40 (2006) 4765.
[18] H.K. Singh, M. Muneer, D. Bahnemann, J. Adv. Oxd. Technol. 7 (2004) 184.
[19] M. Muneer, M. Qamar, M. Saquib, D. Bahnemann, Chemosphere 61 (2005) 457.
[20] H.K. Singh, M. Saquib, M.M. Haque, M. Muneer, D.W. Bahnemann, J. Hazard. Mater. 142 (2007) 374.
[21] H.K. Singh, M. Saquib, M.M. Haque, M. Muneer, D.W. Bahnemann, J. Mol. Catal. A: Chem. 264 (2007) 66.
[22] M.M. Haque, M. Muneer, Dyes Pigments, in press.
[23] R.I. Bickley, T.G. Carreno, J.S. Lees, L. Palmisano, R.J.D. Tilley, J. Solid State Chem. 92 (1992) 178.
[24] M. Lindner, D. Bahnemann, B. Hirthe, W.D. Griebler, J. Sol. Energy Eng. 119 (1997) 120.
[25] S. Rauer, Untersunchung von kommerziell erhaltlichen Titandioxiden hinsichtlich ihrer photokatalytischen Aktivtat, Diplomarbeit, fachhochschule Hannover, Fachbereich Maschinenbau Vertiefung Umwelt- und Verfahrenstechnil, Hannover, Germany, 1998.
[26] D.C. Hurum, A.G. Agrios, K.A. Gray, T. Rajh, M.C. Thurnauer, J. Phys. Chem. B 107 (2003) 4545.
[27] J. Augustynski, Structural Bonding, Springer, Berlin, New York, 1988, p. 69 (Chapter 1).
[28] H. Al-Ekabi, N. Serpone, in: N. Serpone, E. Pellizetti (Eds.), Photocatalysis. Fundamentals and Application, Wiley Interscience, New York, 1989, p. 457.
[29] F. Sabin, T. Turk, A. Vogler, J. Photochem. Photobiol. A: Chem. 63 (1992) 99.
[30] K.W. Krosley, D.M. Collard, J. Adamson, M.A. Fox, J. Photochem. Photobiol. A: Chem. 69 (1993) 357.
[31] K.E. ÒShea, I. Garcia, M. Aguilar, Res. Chem. Intermed. 23 (1997) 325.
[32] M. Qamar, M. Saquib, M. Muneer, Desalination 171 (2004) 185.
[33] H.K. Singh, M. Muneer, D. Bahnemann, Photochem. Photobiol. Sci. 2 (2003) 151.
[34] D.R. Lide (Ed.), Handbook of Chemistry and Physics, seventy sixth ed., CRC Press, London, 1995.
[35] P. Wardman, J. Phys. Chem., Ref. Data 18 (1989) 1657.
[36] M. Muneer, J. Theurich, D. Bahnemann, Res. Chem. Intermed. 25 (1999) 667.
[37] M. Linder, Ph.D. Thesis, Department of Chemistry, University of Hannover, Hannover, Germany, 1997.
[38] G.R. Peyton, W.H. Glaze, Environ. Sci. Technol. 22 (1988) 761.